TECHNICAL RESEARCH REPORT

Convergence Analysis and Analog Circuit Applications for a Class of Networks of Nonlinear Coupled Oscillators

by E.W. Justh, P.S. Krishnaprasad, F.J. Kub

T.R. 96-37

ISR

INSTITUTE FOR SYSTEMS RESEARCH

CONVERGENCE ANALYSIS AND ANALOG CIRCUIT APPLICATIONS FOR A CLASS OF NETWORKS OF NONLINEAR COUPLED OSCILLATORS

Eric W. Justh
SFA, Inc. and the
University of Maryland
at College Park
A.V. Williams Bldg.
College Park MD 20742
justh@eng.umd.edu

P.S. Krishnaprasad
Institute for Systems Research
& Dept. of Electrical Engineering
University of Maryland at College Park
A.V. Williams Bldg. Room 2233
College Park MD 20742
krishna@isr.umd.edu

Francis J. Kub
Code 6813
Naval Research Laboratory
4555 Overlook Ave, SW
Washington DC 20375
kub@estd.nrl.navy.mil

Abstract

The physical motivation and rigorous proof of convergence for a particular network of nonlinear coupled oscillators are reviewed. Next, the network and convergence proof are generalized in several ways, to make the network more applicable to actual engineering problems. It is argued that such coupled oscillator circuits are more natural to implement in analog hardware than other types of dynamical equations because the signal levels tend to remain at sufficiently large values that effects of offsets and mismatch are minimized. Examples of how analog implementations of these networks are able to address actual control problems are given. The first example shows how a pair of coupled oscillators can be used to compensate for the feedback path phase shift in a complex LMS loop, and has potential application for analog adaptive antenna arrays or linear predictor circuits. The second example shows how a single oscillator circuit with feedback could be used for continuous wavelet transform applications. Finally, analog CMOS implementation of the coupled oscillator dynamics is briefly discussed.

1. Introduction

Networks of coupled oscillators have been proposed for various applications, including locomotion (specifically, central pattern generators) [1], pattern recognition (for instance, distinguishing between different objects in view simultaneously), and biological information processing (as a solution to the dynamic binding problem [2,3,4,5]). There is evidence that coupled oscillator networks play a role in biological systems [6], but the point of view taken in this work is that the mathematical analysis of coupled oscillator networks can also yield networks which are useful in their own right for applications in pattern recognition and control. In particular, coupled oscillator networks, with their generally large and predictable signal levels, appear to be better suited to analog VLSI implementation than other dynamical systems because offset and mismatch problems, which lead to large relative errors at small signal levels, are minimal at large signal levels.

The basic network examined in this paper is given by

$$
\begin{aligned}
\dot{y}_j &= -y_j + r(\beta|x_j|)\frac{x_j}{|x_j|} \\
x_j &= \sum_{k=1}^{n} y_k w_{jk}^*, \quad j = 1, ..., n
\end{aligned}
\tag{1}
$$

where x_j and y_j are complex numbers $\forall j$, w_{jk} are fixed complex interconnecting weights with $w_{jj} = 0$ $\forall j$ and $w_{jk} = w_{kj}^*$ (i.e., the weight matrix is Hermitian), β is a scalar parameter, and $r(\cdot) : [0, \infty) \to \Re$ is a memoryless strictly monotone increasing nonlinearity with $r(0) = 0$ and $\lim_{m \to \infty} r(m) = 1$ (later to be specified precisely) [8]. $r(\cdot)$ is also assumed to be analytic, and the function $r(\beta|z|)\frac{z}{|z|} : \mathbb{C} \to \mathbb{C}$ is a well-defined function which compresses the magnitude of its complex argument while retaining its angle.

For the jth unit (or oscillator), y_j may be thought of as its state, and x_j represents its input from the rest of the network. Because the states are complex, each unit carries both phase and amplitude information, and it is the phase information which is of primary interest. In the coupled oscillator context, the phases of coupled oscillators oscillating at the same frequency are represented.

The reason for choosing these dynamical equations is that they represent a very simple method of defining a coupled-oscillator network. The input to each unit is the weighted sum of the states of the other units, where the weights themselves are complex (and thus may alter the phase as well as the amplitude of the signals they weight). The input to each unit is then passed through a memoryless saturating nonlinearity whose gain is a parameter, and the result is then low-pass-filtered to produce that unit's state.

It turns out that the oscillator network described by (1) can be derived from a mean-field analysis of a stochastic physical oscillator problem, as discussed by Zemel, et. al. [8]. Furthermore, the physical motivation leads to a Lyapunov function which can be used to rigorously prove stability of the network, in the sense that every trajectory must converge to an equilibrium point in the ambient space $\Re^{2n}$ in which the complex $x_j, \quad j = 1, ..., n$, evolve [9,10].

However, to proceed further, careful examination of the form of the Lyapunov function is required. The main contribution of this work is an explanation of three ways in which the dynamical equations can be modified, but for which the Lyapunov function can also be modified to retain the convergence property. With these generalizations, the coupled oscillator network is much better suited to potential real-world applications.

With the convergence analyses complete, the focus turns next to simple examples illustrating how such networks can be usefully applied to high-speed analog circuit problems. The first example shows how a pair of coupled oscillators can be used to compensate for the feedback path phase shift in a complex LMS loop, and has potential application for analog adaptive antenna arrays or linear predictor circuits. The second example shows how a single oscillator circuit with feedback could be used for continuous wavelet transform applications. Finally, analog CMOS implementation of the coupled oscillator dynamics is briefly discussed. Application of nonlinear coupled oscillator theory to high-speed analog circuits is a recent development [11,12].

3

2. Fixed-Weight Network Analysis

2.1 Introduction

The dynamics given by (1) can be rewritten solely in terms of the x_j variables:

$$
\begin{aligned}
\dot{x}_j &= \sum_k \dot{y}_k w_{jk}^* \\
&= \sum_k \left(-y_k + r(\beta|x_k|)\frac{x_k}{|x_k|} \right) w_{jk}^* \\
&= -\sum_k y_k w_{jk}^* + \sum_k r(\beta|x_k|)\frac{x_k}{|x_k|} w_{jk}^* \\
&= -x_j + \sum_k r(\beta|x_k|)\frac{x_k}{|x_k|} w_{jk}^*.
\end{aligned}
\tag{2}
$$

These dynamics were proposed and physically motivated by Zemel, et. al. [8]; however, their proof of convergence was incomplete. After a review of the physical motivation, a rigorous proof of convergence, in the sense that each trajectory asymptotically converges to an equilibrium point of the dynamics, will be presented (see, for earlier versions, [9,10]). Furthermore, it is shown that convergence of (2) implies convergence of (1), even if the weight matrix is not invertible.

2.2 Physical Motivation

Zemel, et. al. propose first a stochastic network of directional units (complex-valued random variables with magnitude one and angle representing directional information) interconnected by complex weights which are considered fixed [8]. The directional units evolve according to probability distributions determined by the other directional units and interconnecting weights. The stochastic network is then simplified using the mean-field approximation to give a deterministic network. The purpose of examining the stochastic network is that it provides insight for the stability analysis of the deterministic network.

To begin the stochastic network analysis, consider a network of directional units, each represented by a random variable Z_j taking values on the unit circle in the complex plane. The directional units are interconnected by fixed complex weights w_{jk} satisfying $w_{jj} = 0$ and

$w_{kj} = w^*_{jk}$. Defining $x_j = \sum_k z_k w^*_{jk}$ to represent the interaction of unit j with the rest of the network, the angle of x_j is related to the mean value of Z_j, and the magnitude of x_j is inversely related to the variance of Z_j (the precise dependence to be determined below).

Next, a quadratic form representing "energy" in terms of unit states and interconnecting weights is defined:

$$E(\mathbf{z}) = -\frac{1}{2}\mathbf{z}^T \mathbf{W} \mathbf{z}^* = -\frac{1}{2}\sum_{j,k} z_j z^*_k w_{jk}, \quad \mathbf{z} = (z_1, ..., z_n)^T. \tag{3}$$

Because $\mathbf{W}$ is hermitian (i.e., $w_{kj} = w^*_{jk}$), $E(\mathbf{z})$ is real-valued. (This definition of energy generalizes the Hopfield energy function for binary units [8].) Using $x_j = \sum_k z_k w^*_{jk}$ and changing to polar coordinates: $x_j = a_j e^{i\alpha_j}$ and $z_j = e^{i\phi_j}$ (recall that $|z_j|$ is constrained to equal 1), we define

$$
\begin{aligned}
E_j(\mathbf{z}) &= -\frac{1}{2}\left[z_j x^*_j + (z_j x^*_j)^* \right] \\
&= -a_j \cos(\phi_j - \alpha_j) \tag{4}
\end{aligned}
$$

as unit j's contribution to the total energy. Then $E(\mathbf{z}) = \frac{1}{2}\sum_j E_j(\mathbf{z})$. (Observe that when the angle of x_j is aligned with the angle of z_j, unit j is in a low-energy state.) Introducing a "Boltzmann factor" β (interpreted as the reciprocal of temperature), and taking the probability density that the jth unit is in a state $z_j = e^{i\phi_j}$ to be proportional to $e^{-\beta E_j(\mathbf{z})}$, we obtain:

$$f_{Z_j}(z_j) \propto e^{\beta a_j \cos(\phi_j - \alpha_j)}, \tag{5}$$

where Z_j, the state of unit j, is a random variable taking values on the unit circle in the complex plane and $f_{Z_j}(\cdot)$ is a probability density function. Appropriate normalization gives

$$f_{Z_j}(\phi_j) = \frac{1}{2\pi I_0(m_j)} e^{m_j \cos(\phi_j - \bar\phi_j)}, \quad m_j = \beta a_j, \quad \bar\phi_j = \alpha_j, \tag{6}$$

where $I_0(\cdot)$ is the modified Bessel function of the first kind and order zero. This is known as the Von Mises, or circular normal, distribution, and it is a distribution for circular random variables having some characteristics similar to the usual normal distribution for linear random variables [13]. A circular normal distribution is completely characterized by two parameters: a mean

direction $\bar{\phi} \in [0, 2\pi)$ and a concentration parameter $m > 0$ which corresponds to the reciprocal of the variance of a linear normal random variable.

Next, Zemel, et. al. apply a mean-field approximation to come up with a deterministic network model. In the mean-field approximation, the random variables Z_j are replaced by their means $y_j = <Z_j>$ and are treated as independent (even though they are, in fact, highly coupled). The mean $<Z_j>$ of a Von Mises random variable is a complex number $y_j = r_j e^{i\gamma_j}$ with $\gamma_j = \bar{\phi}_j$ and $r_j = \frac{I_1(m_j)}{I_0(m_j)}$. Figure 2.1 shows r_j as a function of m_j: it is strictly monotone increasing, passes through the origin, and satisfies $\lim_{m_j \to \infty} r_j(m_j) = 1$.
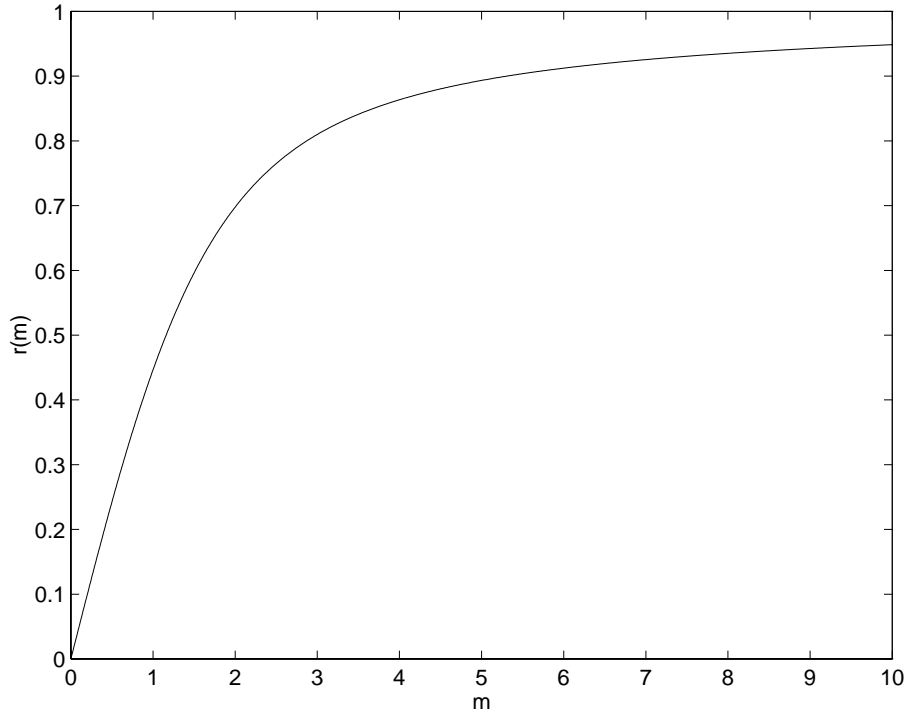

Figure 2.1: Plot of $r_j = \frac{I_1(m_j)}{I_0(m_j)}$ (from [5]).

The dynamics for the deterministic network are chosen to be

$$\frac{dx_j}{dt} = -x_j + \sum_k y_k w_{jk}^*$$ (7)

so that at equilibrium, $x_j = \sum_k y_k w_{jk}^*$, in analogy with the expression $x_j = \sum_k z_k w_{jk}^*$ for the stochastic network. Furthermore, $y_j = r(\beta|x_j|)\frac{x_j}{|x_j|}$, so that if x_j is viewed as determining the

mean and concentration parameter of a Von Mises distribution according to (6), y_j will be the mean value of the distribution. The deterministic dynamics can be expressed in terms of the x_j alone as:

$$\frac{dx_j}{dt} = -x_j + \sum_k r(\beta|x_k|)\frac{x_k}{|x_k|}w_{jk}^*. \tag{8}$$

The total energy for the deterministic network is found by taking the mean of the total energy expression for the stochastic network (and assuming the units are independent):

$$<E> = -\frac{1}{2}\sum_{j,k} y_j y_k^* w_{jk}. \tag{9}$$

Furthermore, the "entropy" for the deterministic network is found by summing the entropies of the individual units of the stochastic network (again using the independence assumption):

$$H = \sum_j \left[-\beta a_j \frac{I_1(\beta a_j)}{I_0(\beta a_j)} + \log(2\pi I_0(\beta a_j)) \right]. \tag{10}$$

With these definitions of $<E>$ and H, a Lyapunov function corresponding to what Zemel et. al. call "free energy," $F = <E> - TH$, $T = \frac{1}{\beta}$, can be computed, and this Lyapunov function can be used to prove convergence of the deterministic network using LaSalle's invariance principle.

2.3 Proof of Convergence

As will now be shown, the deterministic dynamics (2) are convergent: every trajectory converges to an equilibrium point. LaSalle's invariance principle is invoked to prove this, and a Lyapunov function based on the physically motivated "free energy" is used.

Letting $x_j^R = Re(x_j)$ and $x_j^I = Im(x_j)$ we can rewrite the dynamics as

$$\begin{aligned}
\dot{x}_j^R &= -x_j^R + \sum_k r(\beta|x_k|)\frac{x_k^R w_{jk}^R + x_k^I w_{jk}^I}{|x_k|} \\
\dot{x}_j^I &= -x_j^I + \sum_k r(\beta|x_k|)\frac{x_k^I w_{jk}^R - x_k^R w_{jk}^I}{|x_k|}, \quad j = 1,...,n,
\end{aligned} \tag{11}$$

which gives a well-defined vector field on $\Re^{2n}$, the state space for purposes of the proof of convergence. (If $x_k = 0$, we take $r(\beta|x_k|)\frac{x_k^R w_{jk}^R + x_k^I w_{jk}^I}{|x_k|} = r(\beta|x_k|)\frac{x_k^I w_{jk}^R - x_k^R w_{jk}^I}{|x_k|} = 0$.) The equilibrium points of the dynamics are points where $\dot{x}_1^R = \dot{x}_1^I = ... = \dot{x}_n^R = \dot{x}_n^I = 0$.

At any point in the state space $\Re^{2n}$, except where x_j^R and x_j^I are both zero for some j, we can define a valid (nonsingular) change of coordinates by $x_j^R + ix_j^I = a_j e^{i\alpha_j}$, $j = 1, ..., n$. In the new coordinates, the dynamics become:

$$
\begin{aligned}
\dot{a}_j &= -a_j + \sum_k r(\beta a_k)b_{jk}\cos(\alpha_k - \alpha_j - \theta_{jk}) \\
\dot{\alpha}_j &= \frac{1}{a_j}\sum_k r(\beta a_k)b_{jk}\sin(\alpha_k - \alpha_j - \theta_{jk}),
\end{aligned}
\tag{12}
$$

where $w_{jk}^R + iw_{jk}^I = b_{jk}e^{i\theta_{jk}}$.

At all points in $\Re^{2n}$ where the change of coordinates is valid, we define the Lyapunov function (simply the free energy $<E>-TH$, $T = \frac{1}{\beta}$):

$$
\begin{aligned}
V &= -\sum_{j<k} r(\beta a_j)r(\beta a_k)b_{jk}\cos(\alpha_k - \alpha_j - \theta_{jk}) \\
&\quad -T\sum_j \left[-\beta a_j r(\beta a_j) + \log\left(2\pi I_0(\beta a_j)\right)\right]
\end{aligned}
\tag{13}
$$

where log denotes the natural log. (Keep in mind that $w_{jk} = w_{kj}^*$, $w_{jj} = 0$, and $\beta = \frac{1}{T}$.) It turns out that V can be continuously defined even where the change of coordinates is singular, because if either a_j or a_k is taken to be zero in the above formula for V, the term $r(\beta a_j)r(\beta a_k)b_{jk}\cos(\alpha_k - \alpha_j - \theta_{jk})$ will be zero regardless of the value of α_j or α_k. Let $\nu_i = a_i$, $i = 1, 2, ..., n$ and $\nu_{i+n} = \alpha_i$, $i = 1, 2, ..., n$.

Calculating $\dot{V}(\nu) = \frac{\partial V}{\partial \nu}\dot{\nu}$, we obtain

$$
\begin{aligned}
\dot{V}(\nu) &= -\sum_j \left\{ \beta r'(\beta a_j)\left[-a_j + \sum_k r(\beta a_k)b_{jk}\cos(\alpha_k - \alpha_j - \theta_{jk})\right]^2 \right. \\
&\quad \left. + \frac{r(\beta a_j)}{a_j}\left[\sum_k r(\beta a_k)b_{jk}\sin(\alpha_k - \alpha_j - \theta_{jk})\right]^2 \right\}.
\end{aligned}
\tag{14}
$$

8

Note that $r(\beta a_j) > 0 \quad \forall a_j > 0$ and $\frac{r(\beta a_j)}{a_j} > 0 \quad \forall a_j > 0$. Also, $r'(\beta a_j) \to \frac{1}{2}$ as $a_j \to 0$, and $\frac{r(\beta a_j)}{a_j} \to \beta r'(\beta a_j)$ as $a_j \to 0$.

Thus, $\dot{V}(\nu) \leq 0 \quad \forall a_j > 0 \quad \forall \alpha_j$, and $\dot{V}(\nu) = 0$ if and only if

$$\begin{cases} -a_j + \sum_k r(\beta a_k) b_{jk} \cos(\alpha_k - \alpha_j - \theta_{jk}) = 0 \\ \sum_k r(\beta a_k) b_{jk} \sin(\alpha_k - \alpha_j - \theta_{jk}) = 0 \end{cases} \quad \forall j = 1, ..., n. \tag{15}$$

But this will hold at a point $x_j = a_j e^{i\alpha_j} \quad \forall j$ where the change of coordinates is valid if and only if it is an equilibrium point of the dynamics.

We now show that the Lyapunov function $V(\nu)$ has bounded sublevel sets, because this will enable us to exhibit compact sets which are positively invariant under the dynamics, as required to apply LaSalle's invariance principle. Observe that the first term of V,

$$-\sum_{j<k} r(\beta a_j) r(\beta a_k) b_{jk} \cos(\alpha_k - \alpha_j - \theta_{jk}), \tag{16}$$

is bounded as $a_j \to \infty$ for any (or all) a_j. A straightforward but lengthy calculation shows that $\beta a_j r(\beta a_j) - \log(2\pi I_0(\beta a_j)) \to \infty$ as $a_j \to \infty$. Then because $\beta a_j r(\beta a_j) - \log(2\pi I_0(\beta a_j)) > 0 \quad \forall a_j > 0$, and because the terms $\beta a_j r(a_j) - \log(2\pi I_0(\beta a_j))$ appear summed in V, it follows immediately that V is radially unbounded in the a_j (where by definition $V : \Re^n \to \Re$ is radially unbounded in its argument $a \in \Re^n$ if $V(a) \to \infty$ as $||a|| \to \infty$ [14]). Moreover, since V is continuous even at points where the change of coordinates is singular, we can conclude that V has bounded sublevel sets when viewed as a function of $(x_1^R, x_1^I, ..., x_n^R, x_n^I)$.

So far we have shown that there is a Lyapunov function V continuous on all of $\Re^{2n}$, which has bounded sublevel sets, and which has $\dot{V}(\nu) < 0$ provided ν is not an equilibrium point and provided ν is not a point where our change of coordinates is singular. What we will now show is that there is no loss of generality in assuming that a trajectory will pass through points where the change of coordinates is singular only at isolated points in time.

Specifically, we will show that if a trajectory has $x_j^R(t^*) = x_j^I(t^*) = 0$ for some $j \in \{1, ..., n\}$ and for some t^* then either t^* is an isolated point in time for which $x_j^R = x_j^I = 0$ or else

$x_j^R = x_j^I = 0 \ \forall t > 0$. If $x_j^R = x_j^I = 0 \ \forall t > 0$, then simply eliminate the x_j^R and x_j^I coordinates and consider the reduced system of dimension $\Re^{2n-2}$. Repeating this test will reduce the system to a new system with coordinates $(\hat{x}_1^R, \hat{x}_1^I, ..., \hat{x}_{\hat{n}}^R, \hat{x}_{\hat{n}}^I)$ with $\hat{n} \leq n$. The trajectories of the reduced system will have $\hat{x}_j^R(t^*) = \hat{x}_j^I(t^*) = 0$ only at isolated time instants t^*, and hence we will have $\dot{V} = 0$ only at equilibrium points and at isolated times t^*. (It is easy to verify that the reduced system has exactly the same form in terms of dynamics, equilibria, and Lyapunov function as the original system.)

Analyticity properties are the key to showing that the system can be reduced so that $x_j^R = x_j^I = 0$ for some j only at isolated points in time. That the right-hand-side of the differential equation for $(x_1^R(t), x_1^I(t), ..., x_n^R(t), x_n^I(t))$, equation (11), is analytic in the variables $x_1^R, x_1^I, ..., x_n^R, x_n^I$ follows straightforwardly from basic properties of analyticity (using methods in, e.g., [15]). This in turn implies that the trajectory $(x_1^R(t), x_1^I(t), ..., x_n^R(t), x_n^I(t))$ is an analytic function of t (the necessary results on analyticity and differential equations can be found in [16]). Therefore, for any $j \in \{1, ..., n\}$, (x_j^R, x_j^I) will be an analytic function of t. Hence if $x_j^R(t^*) = x_j^I(t^*) = 0$ then either t^* is an isolated point in time for which $x_j^R = x_j^I = 0$ or else $x_j^R = x_j^I = 0 \ \forall t > 0$.

We have a well-defined, C^∞ (in fact, analytic) vector field (11) on $\Re^{2n}$ and a Lyapunov function V which has bounded sublevel sets. For simplicity, think of the vector field abstractly, as given by $\dot{\nu} = f(\nu)$, with Lyapunov function $V(\nu)$. Also, $\dot{V}(\nu) \leq 0$ along trajectories.

Fix $c > 0$ and let

$$\Omega_c = \{\nu \in \Re^{2n} | V(\nu) \leq c\}. \tag{17}$$

In order to apply LaSalle's invariance principle, the chief control theory tool which applies to this problem, we need to show that Ω_c is a compact positively invariant set. We have already shown that the Lyapunov function has bounded sublevel sets, and hence Ω_c is bounded. In fact, it can be easily shown that Ω_c is closed as well, and hence is compact. Positive invariance of Ω_c follows from the fact that $\dot{V}(\nu) \leq 0$ along trajectories.

Theorem 2.1 (LaSalle's invariance principle): Let Ω be a compact set and suppose the solution $\nu(t)$ starting in Ω stays in Ω for all $t > 0$. Let $V : \Omega \to \Re$ be a continuous function such that $V(\nu(t))$ is a monotone nonincreasing function of t. Let E be the set of all points in Ω where $\dot{V}(\nu)$ exists and equals zero. Let M be the largest invariant set in E. Then $\nu(t)$ approaches M as $t \to \infty$.

Proof: (See [14].)

Theorem 2.2: The dynamics (11) converge to an equilibrium point.

Proof: For any initial condition ν_0, reduce the system if necessary so that we may assume that the coordinate transformation is only singular at isolated points in time. Also, choose $c > 0$ to be greater than or equal to $V(\nu_0)$. Then the set Ω in Theorem 2.1 is taken to be Ω_c, as defined earlier, which is a well-defined compact subset of $\Re^{2n}$ when viewed in $(x_1^R, x_1^I, ..., x_n^R, x_n^I)$ coordinates. Because the vector field is well-defined, the Lyapunov function is monotone nonincreasing along trajectories, and the set Ω_c is compact, it follows that the trajectory $\nu(t)$ exists and stays in Ω_c $\forall t > 0$. Thus, the hypotheses of Theorem 2.1 are satisfied, enabling us to conclude that the trajectory will converge to the largest invariant subset of the set of points in Ω_c such that $\dot{V}(\nu) = 0$. But the largest invariant subset of the set of points with $\dot{V}(\nu) = 0$ are just the equilibrium points of the system which lie inside Ω_c.

LaSalle's Principle thus enables us to conclude convergence of any trajectory to the set of equilibrium points of the dynamics, but not to a specific equilibrium point. We will now show, by appropriate choice of inner product, that the system follows gradient dynamics except at isolated points in time. At points $\nu = (a_1, ..., a_n, \alpha_1, ..., \alpha_n)$, define the inner product:

$$\left\langle v_\nu^1, v_\nu^2 \right\rangle = v_\nu^{1\,T} \mathrm{diag}(\beta r'(\beta a_1), ..., \beta r'(\beta a_n), a_1 r(\beta a_1), ..., a_n r(\beta a_n)) v_\nu^2, \qquad (18)$$

where v_ν^1 and v_ν^2 are two tangent vectors at the point ν. Then $\langle \dot{\nu}, v_\nu \rangle = -d_\nu V \cdot v_\nu = \langle -\nabla V, v_\nu \rangle$ so that $\dot{\nu} = -\nabla V$; i.e., the system satisfies gradient dynamics (except at isolated time instants). Thus, we may conclude that in fact the dynamics (11) converge to an equilibium point. Q.E.D.

2.3 Application of Convergence Result

The convergence result just proved implies the convergence of the complex dynamics (2). An additional argument is required to conclude that the dynamics of equation (1) converge. Because the x_j converge to constant values, the terms

$$u_j = r(\beta|x_j|)\frac{x_j}{|x_j|} \tag{19}$$

also converge to constant values (by continuity). Now consider the system

$$\dot{y}_j = -y_j + u_j, \tag{20}$$

which is clearly globally asymptotically stable if the u_j are constant. Because the x_j trajectories remain bounded, so do the u_j, and it is not hard to see that the u_j remaining bounded implies that the y_j trajectories also remain bounded. Therefore, the y_j asymptotically converge to an equilibrium point [17].

2.4 Generalization to a Class of Networks

Although the choice of $r(\cdot)$ as the ratio of bessel functions enabled a physical motivation to be given for the dynamics, careful examination of the proof of convergence reveals that as long as $r(\cdot)$ satisfies certain properties, the convergence result will still hold. First, the function $r(\cdot)$ must be strictly monotone increasing with $r(0) = 0$. Second, $r(\cdot)$ must be analytic. Third, we need to ensure that a suitable radially unbounded Lyapunov function exists:

$$V = -\sum_{j<k} r(a_j)r(a_k)b_{jk}\cos(\alpha_k - \alpha_j - \theta_{jk}) + \sum_j h(a_j) \tag{21}$$

where $\lim_{a\to\infty} \frac{h(a)}{r^2(a)} = \infty$, $\frac{\partial h}{\partial a} = ar'(a)$, and $h(0) = $ constant.

The ability to generalize the convergence proof to a class of networks in this manner is important when analog implementations of these networks are considered. Although saturating nonlinearities can be achieved in analog hardware, a saturating nonlinearity for the magnitude of a complex number which leaves the phase unaltered is more complicated [9].

3. Adaptive Control Law for a Variable-Weight Network

3.1 Motivation for the Adaptive Control Law

The usefulness of the network presented in the last section would be greatly enhanced if the weights were not constrained to be constant. An adaptive control law for variable weights is now described which retains the convergence properties of the fixed-weight network - namely, the variable weight network with adaptively controlled weights is shown to converge to an equilibrium point. The utility of the rigorous proof of convergence for the fixed-weight network is that it can be extended to more general and useful networks, of which the adaptive control law described here is an example.

The mathematical motivation for the adaptive control law comes from viewing the dynamics and Lyapunov function abstractly and performing some calculations. Abstractly, for the fixed-weight case we have

$$\dot{\nu} \;=\; f(\nu, w) \;\; \text{(dynamics)}$$

$$V(\nu, w) \qquad \text{(Lyapunov function)}$$

$$\dot{V}(\nu, w) \;=\; \frac{\partial V}{\partial \nu} f(\nu, w)$$

$$\;=\; - < f(\nu, w), f(\nu, w) > . \tag{22}$$

Now letting some of the weights be feedback functions, we have

$$\dot{\nu} \;=\; f(\nu, w(\nu)) + g(\nu) \;\; \text{(dynamics)}$$

$$V(\nu, w(\nu)) \qquad \text{(Lyapunov function)}$$

$$\dot{V}(\nu, w(\nu)) \;=\; \left(\frac{\partial V}{\partial \nu} + \frac{\partial V}{\partial w}\frac{\partial w}{\partial \nu} \right) (f(\nu, w(\nu)) + g(\nu))$$

$$\;=\; - < f(\nu, w(\nu)) + g(\nu), f(\nu, w(\nu)) + g(\nu) > \tag{23}$$

provided

$$\left(\frac{\partial V}{\partial w}\frac{\partial w}{\partial \nu} \right) \eta = - < g(\nu), \eta > . \tag{24}$$

In the transformed coordinates, this condition becomes

$$
\frac{\partial V}{\partial w}\frac{\partial w}{\partial \nu} = -[\beta r'(\beta a_1)g_1(\nu)\cdots\beta r'(\beta a_n)g_n(\nu)
$$
$$
a_1 r(\beta a_1)g_{n+1}(\nu)\cdots a_n r(\beta a_n)g_{2n}(\nu)]. \tag{25}
$$

Suppose unit j interconnects units l_1 and l_2, and all other weights are constants. Furthermore, suppose b_{l_1,l_2} depends only on a_j and θ_{l_1,l_2} depends only on α_j. Then for V as in (13),

$$
\frac{\partial V}{\partial w}\frac{\partial w}{\partial \nu} = \Big[0\cdots0 \ -r(\beta a_{l_1})r(\beta a_{l_2})\frac{\partial b_{l_1,l_2}}{\partial a_j}\cos(\alpha_{l_2}-\alpha_{l_1}-\theta_{l_1,l_2}) \ 0\cdots0
$$
$$
0\cdots0 \ -r(\beta a_{l_1})r(\beta a_{l_2})b_{l_1,l_2}\sin(\alpha_{l_2}-\alpha_{l_1}-\theta_{l_1,l_2})\frac{\partial \theta_{l_1,l_2}}{\partial \alpha_j} \ 0\cdots0\Big] \tag{26}
$$

where the first nonzero term is in position j of the row vector, and the second nonzero term is in position $j+n$.

If we choose $b_{l_1,l_2}(a_j)=d_{l_1,l_2}r(\beta a_j)$ and $\theta_{l_1,l_2}(\alpha_j)=\alpha_j$, then $\frac{\partial b_{l_1,l_2}}{\partial a_j}=d_{l_1,l_2}\beta r'(\beta a_j)$ and $\frac{\partial \theta_{l_1,l_2}}{\partial \alpha_j}=1$, so

$$
\frac{\partial V}{\partial w}\frac{\partial w}{\partial \nu} = -\Big[0\cdots0 \ \beta r'(\beta a_j)(d_{l_1,l_2}r(\beta a_{l_1})r(\beta a_{l_2})\cos(\alpha_{l_2}-\alpha_{l_1}-\alpha_j)) \ 0\cdots0
$$
$$
0\cdots0 \ a_j r(\beta a_j)\left(\frac{1}{a_j}d_{l_1,l_2}r(\beta a_{l_1})r(\beta a_{l_2})\sin(\alpha_{l_2}-\alpha_{l_1}-\alpha_j)\right) \ 0\cdots0\Big] \tag{27}
$$

where again the nonzero terms are in positions j and $j+n$ of the row vector.

Thus, letting

$$
g_j(\nu) = d_{l_1,l_2}r(\beta a_{l_1})r(\beta a_{l_2})\cos(\alpha_{l_2}-\alpha_{l_1}-\alpha_j)
$$
$$
g_{j+n}(\nu) = \frac{1}{a_j}d_{l_1,l_2}r(\beta a_{l_1})r(\beta a_{l_2})\sin(\alpha_{l_2}-\alpha_{l_1}-\alpha_j)
$$
$$
g_k(\nu) = 0, \ \ k\neq j, j+n \tag{28}
$$

we then have

$$
(\frac{\partial V}{\partial w}\frac{\partial w}{\partial \nu})\eta = -<g(\nu),\eta> . \tag{29}
$$

Generalizing to an arbitrary number of variable weights, we have

$$
I^j_{l_1,l_2} = \begin{cases} 1 & \text{if } b_{l_1,l_2} e^{i\theta_{l_1,l_2}} = d_{l_1,l_2} r(\beta a_j) e^{i\alpha_j} \\ 0 & \text{otherwise} \end{cases}
$$

$$
\dot{a}_j = -a_j + \sum_k r(\beta a_k) b_{jk} \cos(\alpha_k - \alpha_j - \theta_{jk})
$$
$$
+ \sum_{l_1,l_2} I^j_{l_1,l_2} d_{l_1,l_2} r(\beta a_{l_1}) r(\beta a_{l_2}) \cos(\alpha_{l_2} - \alpha_{l_1} - \alpha_j)
$$

$$
\dot{\alpha}_j = \frac{1}{a_j} \Big(\sum_k r(\beta a_k) b_{jk} \sin(\alpha_k - \alpha_j - \theta_{jk})
$$
$$
+ \sum_{l_1,l_2} I^j_{l_1,l_2} d_{l_1,l_2} r(\beta a_{l_1}) r(\beta a_{l_2}) \sin(\alpha_{l_2} - \alpha_{l_1} - \alpha_j) \Big) \tag{30}
$$

which (provided the change of coordinates is nonsingular) is equivalent to

$$
I^j_{l_1,l_2} = \begin{cases} 1 & \text{if } w_{l_1,l_2} = d_{l_1,l_2} r(\beta|x_j|) \frac{x_j}{|x_j|} \\ 0 & \text{otherwise} \end{cases}
$$

$$
\dot{x}_j = -x_j + \sum_k r(\beta|x_k|) \frac{x_k}{|x_k|} w^*_{jk}
$$
$$
+ \sum_{l_1,l_2} I^j_{l_1,l_2} d_{l_1,l_2} r(\beta|x_{l_1}|) r(\beta|x_{l_2}|) \frac{x_{l_2}}{|x_{l_2}|} \frac{x^*_{l_1}}{|x_{l_1}|}, \tag{31}
$$

where the conditions $b_{l_1,l_2} e^{i\theta_{l_1,l_2}} = d_{l_1,l_2} r(\beta a_j) e^{i\alpha_j}$ and $w_{l_1,l_2} = d_{l_1,l_2} r(\beta|x_j|) \frac{x_j}{|x_j|}$ simply indicate that unit j is serving as the interconnecting weight between units l_1 and l_2, with the sense of the connection (recall that $w_{kj} = w^*_{jk}$) taken into account.

3.2 Proof of Convergence for the Adaptive Control Law

To prove convergence of the adaptive control law, we start with the dynamical equations just given, (30)-(31), along with the Lyapunov function

$$
V = -\sum_{j<k} r(\beta a_j) r(\beta a_k) b_{jk} \cos(\alpha_k - \alpha_j - \theta_{jk})
$$
$$
-T \sum_j \left[-\beta a_j r(\beta a_j) + \log\left(2\pi I_0(\beta a_j)\right) \right], \tag{32}
$$

where now we may have $b_{jk} = d_{jk} r(\beta a_l)$ and $\theta_{jk} = \pm\alpha_l$ for various j, k, l.

The new calculation of $\dot{V}$ gives:

$$
\dot{V}(\nu) = -\sum_j \left\{ \beta r'(\beta a_j) \left[-a_j + \sum_k r(\beta a_k) b_{jk} \cos(\alpha_k - \alpha_j - \theta_{jk}) \right.\right.
$$

15

$$+ \sum_{l_1,l_2} I^j_{l_1,l_2} d_{l_1,l_2} r(\beta a_{l_1}) r(\beta a_{l_2}) \cos(\alpha_{l_2} - \alpha_{l_1} - \alpha_j) \Big]^2$$

$$+ \frac{r(\beta a_j)}{a_j} \Big[\sum_k r(\beta a_k) b_{jk} \sin(\alpha_k - \alpha_j - \theta_{jk})$$

$$+ \sum_{l_1,l_2} I^j_{l_1,l_2} d_{l_1,l_2} r(\beta a_{l_1}) r(\beta a_{l_2}) \sin(\alpha_{l_2} - \alpha_{l_1} - \alpha_j) \Big]^2 \Big\}. \tag{33}$$

From this point on, the proof of convergence is basically the same as the convergence proof for the fixed-weight case. The reason for labeling the feedback law an adaptive control law is that the original dynamics were linear in certain parameters (the weights), which are now adapted according to a feedback law which guarantees convergence. In this way, coupled oscillator networks can be designed to adapt in the presence of, for example, fixed but (a priori) unknown weight values.

3.3 Application of the Adaptive Control Law Convergence Result

The adaptive control law just derived is in the form corresponding to equation (2) rather than equation (1) for the fixed-weight case. Therefore, we need to determine how equation (1) should be modified to correspond to equation (31). A calculation (shown in [9]) gives the required modification to (1):

$$\dot{y}_j = -y_j + r(\beta|x_j|)\frac{x_j}{|x_j|}$$

$$x_j = \sum_{k=1}^n y_k w^*_{jk} + u_j - \sum_{l_1,l_2} I^{l_1}_{j,l_2} d_{j,l_2} y_{l_2} r(\beta|x_{l_1}|)\frac{x^*_{l_1}}{|x_{l_1}|}$$

$$\dot{u}_j = -u_j + \sum_{l_1,l_2} \left(I^j_{l_1,l_2} d_{l_1,l_2} + I^{l_1}_{j,l_2} d_{j,l_2} \right) r(\beta|x_{l_1}|) r(\beta|x_{l_2}|)\frac{x_{l_2}}{|x_{l_2}|}\frac{x^*_{l_1}}{|x_{l_1}|}$$

$$y_j = r(\beta|x_j|)\frac{x_j}{|x_j|} \text{ at equilibrium.} \tag{34}$$

An example illustrating how this adaptive control law might be used is discussed in [9,10].

There is an interesting implication of the adaptively controlled network convergence result in terms of hierarchical control of coupled oscillator networks. If two or more networks are arranged in a hierarchical fashion, with the units of one network serving as the weights for the next network in the hierarchy, the convergence result implies that feedback can be applied from

lower levels to higher levels and stability will be maintained, as long as the adaptive control law is obeyed. Consideration of these networks of coupled oscillators for hierarchical control systems with local and global feedback might therefore be worthwhile.

4. Network with Auxiliary Control Inputs

4.1 Convergence Result

Besides adaptively controlling the weights, another way in which it would be useful to extend the basic coupled-oscillator network would be to add auxiliary inputs and determine under what circumstances the network is still guaranteed to converge. So consider adding a control input term to equation (1):

$$
\begin{aligned}
\dot{y}_j &= -y_j + r(\beta|x_j|)\frac{x_j}{|x_j|} \\
x_j &= \sum_{k=1}^{n} y_k w_{jk}^* + u_j, \quad j = 1, ..., n.
\end{aligned}
\tag{35}
$$

Computing the dynamics for the x_j alone, in the manner of equation (2), we find

$$
\dot{x}_j = -x_j + \sum_{k=1}^{n} r(\beta|x_k|)\frac{x_k}{|x_k|} w_{jk}^* + v_j,
\tag{36}
$$

where $v_j = u_j + \dot{u}_j$. Our ambient space, the space in which the trajectories are considered to lie, is still $\Re^{2n}$. Next, we change to polar coordinates using

$$
\begin{aligned}
x_j &= a_j e^{i\alpha_j} \\
w_{jk} &= b_{jk} e^{i\theta_{jk}} \\
v_j &= d_j e^{i\psi_j},
\end{aligned}
\tag{37}
$$

so that the dynamics become

$$
\begin{aligned}
\dot{a}_j &= -a_j + \sum_k r(\beta a_k) b_{jk} \cos(\alpha_k - \alpha_j - \theta_{jk}) + d_j \cos(\psi_j - \alpha_j) \\
\dot{\alpha}_j &= \frac{1}{a_j}\left[\sum_k r(\beta a_k) b_{jk} \sin(\alpha_k - \alpha_j - \theta_{jk}) + d_j \sin(\psi_j - \alpha_j)\right].
\end{aligned}
\tag{38}
$$

17

For now, assume that the v_j are constants instead of functions of time, and at all points in $\Re^{2n}$ where the change of coordinates is valid, consider the new Lyapunov function

$$
\begin{aligned}
V &= -\sum_{j<k} r(\beta a_j) r(\beta a_k) b_{jk} \cos(\alpha_k - \alpha_j - \theta_{jk}) - \sum_j r(\beta a_j) d_j \cos(\psi_j - \alpha_j) \\
&\quad - T \sum_j \left[-\beta a_j r(\beta a_j) + \log\left(2\pi I_0(\beta a_j)\right) \right].
\end{aligned}
\tag{39}
$$

Calculating $\dot{V}(\nu) = \frac{\partial V}{\partial \nu} \dot{\nu}$ (under the assumption that the v_j are constant) gives

$$
\begin{aligned}
\dot{V}(\nu) &= -\sum_j \left\{ \beta r'(\beta a_j) \left[-a_j + \sum_k r(\beta a_k) b_{jk} \cos(\alpha_k - \alpha_j - \theta_{jk}) + d_j \cos(\psi_j - \alpha_j) \right]^2 \right. \\
&\quad \left. + \frac{r(\beta a_j)}{a_j} \left[\sum_k r(\beta a_k) b_{jk} \sin(\alpha_k - \alpha_j - \theta_{jk}) + d_j \sin(\psi_j - \alpha_j) \right]^2 \right\}.
\end{aligned}
\tag{40}
$$

Again, from this point on, the proof of convergence with the v_j constant is essentially the same as in the fixed-weight case.

The convergence result can be extended to the case where u_j and v_j are nonconstant in the following manner. As long as both u_j and $\dot{u}_j$ are bounded, $v_j = u_j + \dot{u}_j$ will also be bounded, and hence for any initial condition, the x_j trajectories will remain bounded. Therefore, as long as v_j asymptotically converges to a constant value, the coupled-oscillator system will asymtotically converge to an equilibrium point [17].

4.2 Example: Feedback Loop Phase Shift Compensating Circuit

4.2.1 Overview of the feedback loop phase shift problem

This example illustrates how the theory of nonlinear coupled oscillators can be applied to a real-world analog circuit problem: phase shift in the feedback path of a complex LMS loop configured as a frequency-programmable bandpass filter. In theory, an ideal frequency-programmable two-pole linear bandpass filter can be implemented using a single complex LMS loop. However, one critical nonideality which must be taken into account at high center frequencies is phase shift through the feedback path due to propagation delays and finite component bandwidths.

Figure 4.1 shows a single-complex-learning-element LMS adaptive filter [18]. The actual circuit used is described in [19]. In the absence of feedback path delays and other nonidealities, by applying a fixed reference frequency to the "oscillator natural frequency" input, the circuit behaves as a bandpass filter from the "exogenous input" to "output" ports. However, for certain values of gain and phase shift through the feedback path, labeled "μ" in figure 1, it is well-known that the LMS loop becomes unstable, in the sense that the feedback becomes positive.
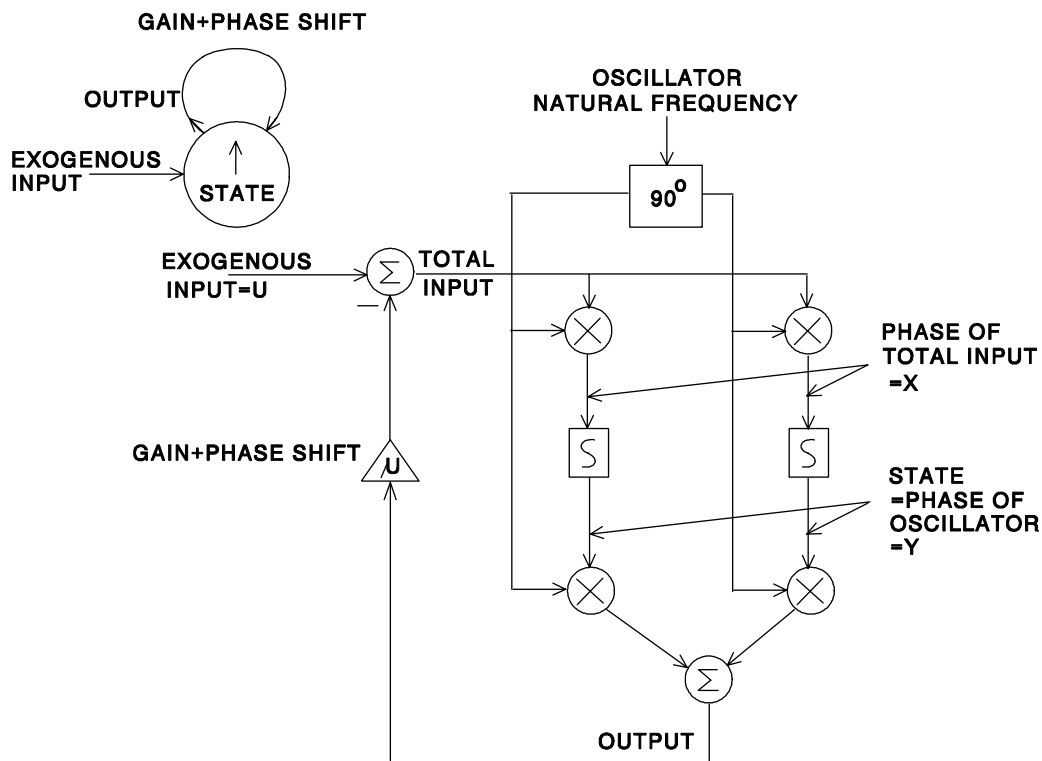

Figure 4.1: Bandpass filter circuit and oscillator representation.

In the upper-left corner of figure 4.1 is a sketch of how the system can be viewed as an oscillator. The oscillator point of view does not distinguish between stability and instability based on whether the feedback is positive or negative. Stability for the LMS model corresponds to a stable equilibrium point at the origin for the oscillator system, and instability for the LMS model corresponds to a stable limit cycle solution for the oscillator system (the amplitude of the oscillations are limited in practice by the range of the analog elements used). To further simplify

the oscillator model, only the oscillator amplitude and phase (relative to the unforced natural frequency) are retained. This information can be compactly modeled as a time-varying vector in the complex plane, and is what is represented by the upward pointing arrow labeled "state" in figure 4.1. As will be demonstrated, the oscillator point of view leads to a simple analysis of how the LMS loop functions as a bandpass filter.

4.2.2 LMS loop bandpass filter mathematical analysis

Each signal in the circuit is represented as a complex-valued function of time with magnitude corresponding to the amplitude of the signal and with angle corresponding to the phase of the signal. If the signal is high-frequency, then its phase is measured with respect to the unforced natural frequency of the oscillator (in this case the bandpass filter programming frequency). The goal is to derive the transfer function from the complex exogenous input to the state, which in turn determines the bandpass filter characteristic from exogenous input to output. (The following analysis is a linearized analysis about the equilibrium point at the origin for the bandpass filter oscillator, and thus only applies when the equilibrium point at the origin is stable.)

Referring to figure 4.1, and treating the integrator block as a single-pole low-pass filter with transfer function $K/(s + \omega_0)$, we have the following differential equation for the oscillator state $y(t)$:

$$\dot{y}(t) = -\omega_0 y(t) + Kx(t), \tag{41}$$

with x(t) is given by

$$x(t) = u(t) - \mu y(t), \tag{42}$$

giving

$$\dot{y}(t) = -(\omega_0 + K\mu)y(t) + Ku(t). \tag{43}$$

Thus, the transfer function from input to state is

$$\begin{aligned} \frac{Y(s)}{U(s)} &= \frac{K}{s + (\omega_0 + K\mu)} \\ &= \frac{K}{s + (\omega_0 + Kbe^{j\theta})}, \end{aligned} \tag{44}$$

where $b = |\mu|$ and $\theta = \angle \mu$.

From this transfer function, we deduce that as the feedback path phase shift increases toward instability for the LMS loop, the bandpass filter center frequency shifts higher in frequency, and the bandwidth of the filter narrows, approaching the bandwidth of the low-pass filters used as the integrators. Also, as the feedback path phase shift increases, the filter gain at the center frequency increases. Clearly feedback path phase shift has a profound effect on the performance of the complex LMS loop as a bandpass filter.

4.2.3 Phase shift compensation circuit

Figure 4.2 shows a modification to the circuit of figure 4.1 to allow an additional compensating phase shift to be incorporated, which could serve to bring the overall loop phase shift to zero.
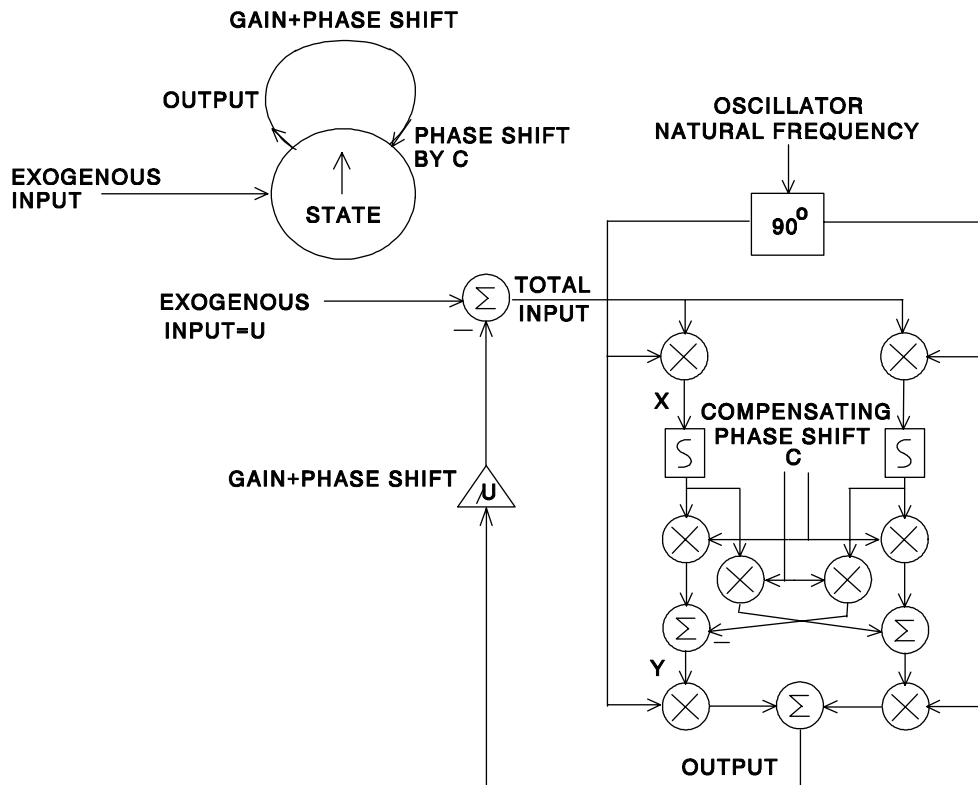

Figure 4.2: Bandpass filter circuit with compensating phase shift.

21

Figure 4.3 shows a nonlinear oscillator diagram for the phase compensation circuit. Oscillators y_1 and y_2 are interconnected so that their stable equilibrium phases differ by the feedback path phase shift, $\angle\mu$. The input u to y_1 is the bandpass filter programming signal, which causes the phase of y_1 to allign with the phase of the programming signal. Therefore, the phase of y_2 converges to the phase of the feedback path phase shift, $\angle\mu$. The phase of y_2 is in turn used to shift the phase of the bandpass filter feedback signal so correct for the $\angle\mu$ phase shift through the feedback path of the bandpass filter LMS loop.
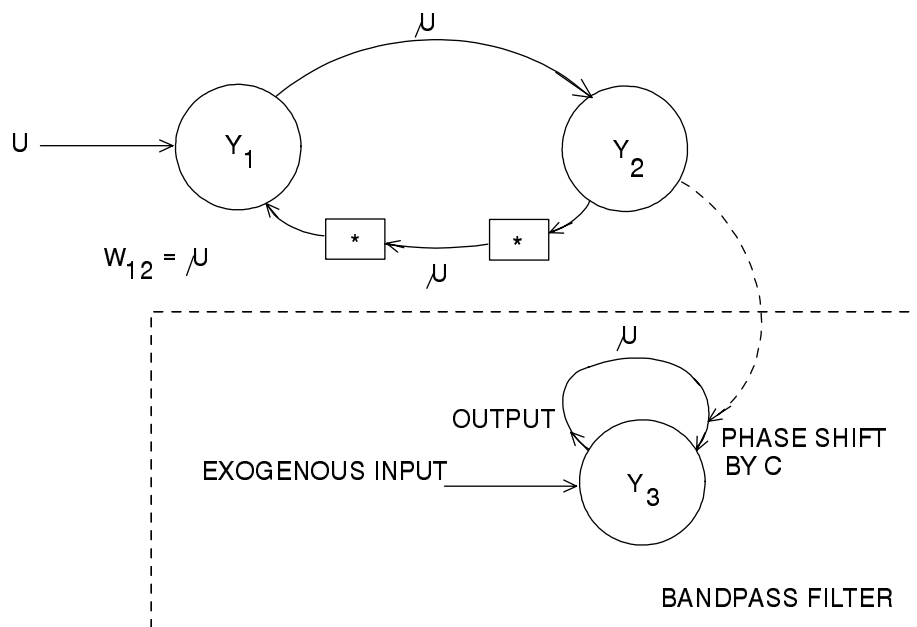

Figure 4.3: Coupled oscillators for compensating bandpass filter feedback phase shift.

Figure 4.4 shows the general schematic for implementing the pair of coupled oscillators y_1 and y_2. As indicated in figure 4.4, complex conjugation simply amounts to a change in sign, and hence with the differential circuits described in [19] implies no additional circuit complexity. Although not shown explicitly in figure 4.4, it is to be understood that the upper row of multipliers, in particular, have a smoothly saturating input characteristic with respect to the input signal from the other oscillator. Although all the analog components have finite range, it is the saturating characteristic of the first multipliers (in the multiply-integrate-multiply chain) which

are assumed to apply the saturating characteristic in the dynamical equations used to describe the coupled oscillator system.
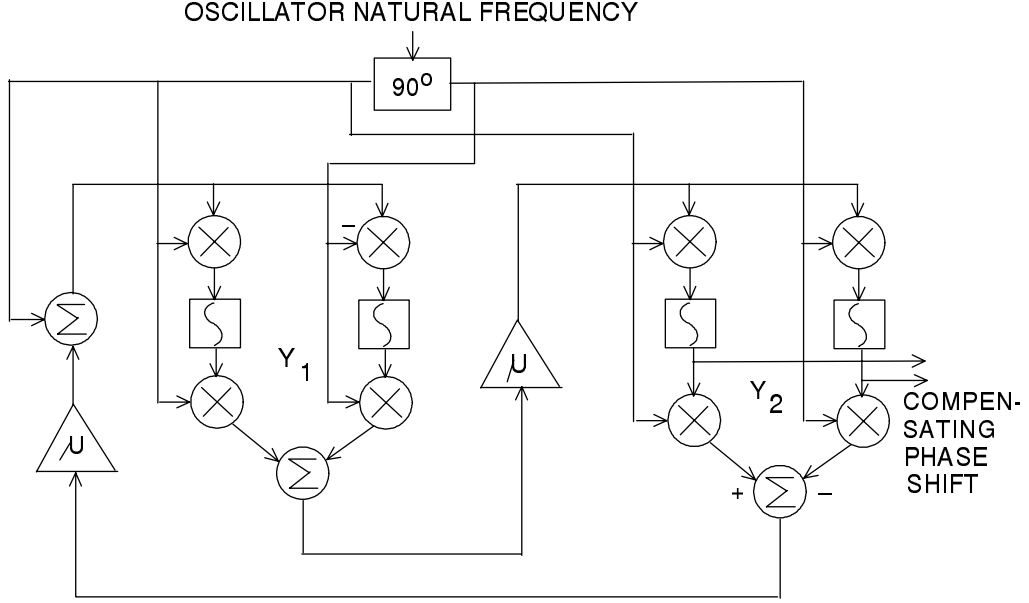

Figure 4.4: Coupled oscillator circuit showing complex conjugation.

The dynamical equations for the coupled oscillators y_1 and y_2 are

$$\begin{aligned}
\dot{y}_1 &= -y_1 + r(\beta|y_2\mu^* + u|)\frac{y_2\mu^* + u}{|y_2\mu^* + u|} \\
\dot{y}_2 &= -y_2 + r(\beta|y_1\mu|)\frac{y_1\mu}{|y_1\mu|},
\end{aligned}$$

(45)

where ω_0 is taken to be 1 for simplicity. By the general stability result of section 4, the oscillator network consisting of y_1 and y_2 will converge to steady-state magnitudes and phases. Changing to the transformed coordinates, if there is no stable equilibrium point with $a_j = 0$ for any j, then we can conclude that the stable steady-state phases of y_1 and y_2 will be included in the set

$$\sum_k r(\beta a_k)b_{jk}\sin(\alpha_k - \alpha_j - \theta_{jk}) + d_j\sin(\psi_j - \alpha_j) = 0,$$

(46)

which in this case reduces to

$$r(\beta a_1)b\sin(\alpha_2 - \alpha_1 - \theta) + d\sin(\psi - \alpha_1) = 0$$

$$r(\beta a_2)b\sin(\alpha_1 - \alpha_2 + \theta) \quad = \quad 0, \tag{47}$$

where $\mu = be^{i\theta}$ and $u = de^{i\psi}$. The desired equilibrium solution is the one for which y_1 is alligned with u and the phase difference between y_1 and y_2 corresponds to the feedback path phase shift of μ:

$$\left(\begin{array}{c} \alpha_1 \\ \alpha_2 \end{array} \right) = \left(\begin{array}{c} \psi \\ \psi + \theta \end{array} \right). \tag{48}$$

The desired equilibrium solution is indeed an equilibrium solution, but there are other equilibrium solutions as well. Futhermore, we must carefully rule out the possibility of a stable equilibrium point with $a_1 = 0$ or $a_2 = 0$. For this simple two-oscillator network, if the steady-state value of u is nonzero, then no equilibrium point has $a_1 = 0$ or $a_2 = 0$. (If the steady state value of u is zero, the equilibrium point at the origin can be destabilized by choosing the gain βb sufficiently large [9].) The technique for showing that the desired equilibrium point is the unique stable equilibrium point uses the Lyapunov function, which for the two-oscillator network becomes

$$\begin{aligned} V \quad = \quad & -r(\beta a_1)r(\beta a_2)b\cos(\alpha_2 - \alpha_1 - \theta) - r(\beta a_1)d\cos(\psi - \alpha_1) \\ & -T[-\beta a_1 r(\beta a_1) + \log(2\pi I_0(\beta a_1)) - \beta a_2 r(\beta a_2) + \log(2\pi I_0(\beta a_2))]. \end{aligned} \tag{49}$$

The equilibrium phases are

$$\begin{aligned} \left(\begin{array}{c} \alpha_1 \\ \alpha_2 \end{array} \right) \quad &= \quad \left(\begin{array}{c} \psi \\ \psi + \theta \end{array} \right) \quad \text{(the desired equilibrium)} \\ \left(\begin{array}{c} \alpha_1 \\ \alpha_2 \end{array} \right) \quad &= \quad \left(\begin{array}{c} \psi + \pi \\ \psi + \pi + \theta \end{array} \right) \\ \left(\begin{array}{c} \alpha_1 \\ \alpha_2 \end{array} \right) \quad &= \quad \left(\begin{array}{c} \psi + \pi \\ \psi + \theta \end{array} \right) \\ \left(\begin{array}{c} \alpha_1 \\ \alpha_2 \end{array} \right) \quad &= \quad \left(\begin{array}{c} \psi \\ \psi + \pi + \theta \end{array} \right). \end{aligned} \tag{50}$$

However, for all but the desired equilibrium point, perturbing the equilibrium angles in the expression for V is seen to reduce V. On the other hand, for the desired equilibrium point, perturbing the equilibrium angles in the expression for V increases V. Hence, the desired equilibrium point is indeed the unique stable equilibrium point.

Now that we have shown that y_1 and y_2 converge appropriately in figure 4.4, with the steady-state phase of y_2 corresponding to the feedback path phase shift of μ, it is clear that applying y_2^* directly to the "compensating phase shift" input to the bandpass filter in figure 4.2 will bring the total loop phase shift to zero. The complex conjugation of y_2 again involves no additional circuit complexity, as it simply amounts to a sign change.

The practical importance of the coupled-oscillator approach to correcting for the feedback path phase shift in the LMS-loop frequency-programmable bandpass filter is that it addresses one of the major limitations of a widely used and important high-speed analog feedback circuit configuration. The frequency-programmable single-complex-LMS-loop bandpass filter is a special case of a more general network architecture, the least-mean-square-error adaptive filter circuit used in adaptive antenna arrays, co-site interference rejection circuits, and linear-predictor circuits for separating coherent from noncoherent signals. Each of these circuits requires feedback, and feedback path phase shift is a major limitation at high frequencies of operation.

One aspect of the feedback path phase shift correction circuit worth emphasizing is that the correct compensating phase is determined regardless of the feedback path phase shift over the full range from zero to 2π. This property indicates that coupled oscillator circuits may prove quite useful for high-speed analog feedback circuit design problems, where signal phase shifts are large and difficult to estimate.

5. Single Feedback Oscillator for Frequency Translation

5.1 Convergence Result

So far, we have generalized the basic fixed-weight network by allowing for an adaptive control law to update some of the complex weights and by allowing for auxiliary inputs. However, in order to guarantee convergence, a key assumption was the Hermitian symmetry of the weight matrix. It turns out that a simplified version of the same basic technique for proving convergence can also be used for a single oscillator feeding back to itself with an arbitrary weight. In fact,

this is precisely the situation in the complex LMS loop with feedback path phase shift: the complex LMS loop with a saturating characteristic in the high-speed feedback path acts as an oscillator with the feedback weight determined by the feedback path phase shift. When used to implement the LMS algorithm, the complex feedback weight must stabilize the equilibrium at the origin, or the circuit is considered "unstable." However, with a feedback path weight value which destabilizes the origin, the circuit is stable in the sense of converging to a stable limit cycle, and this behavior can be employed to translate the natural frequency of the complex LMS loop viewed as an oscillator to a different output frequency determined by the complex weight in the feedback path. One use envisioned for such a circuit is as a reference-frequency generator for a continuous wavelet transform (CWT) circuit.

Figure 5.1 identifies the signals relevant to the oscillator analysis: y is a complex number representing the (low-frequency component of the) input to the low-pass filter, x is a complex number representing the low-pass filter output, and c is the complex input signal (supplied as voltages corresponding to its real and imaginary parts) providing phase shift in the feedback path. (The x and y signals are interchanged with respect to the previous example to simplify the algebra.) The signal y is passed through the lowpass filter with corner frequency ω_0 to produce x, so one equation for the circuit is

$$\frac{1}{\omega_0}\dot{x} = -x + y. \tag{51}$$

The high-frequency positive feedback with sigmoidal nonlinearity acts to amplify the complex signal cx, and saturate its magnitude without altering its phase. This leads to the second equation for the circuit,

$$y = r_\beta(|cx|)\frac{cx}{|cx|}, \tag{52}$$

where β is a real constant and $z \mapsto r_\beta(|z|)\frac{z}{|z|}$ is a complex-valued function which compresses the magnitude of its complex argument while leaving its phase unaltered. The small-signal gain of the saturation function is parameterized by β. Combining these two equations gives

$$\frac{1}{\omega_0}\dot{x} = -x + r_\beta(|cx|)\frac{cx}{|cx|}. \tag{53}$$
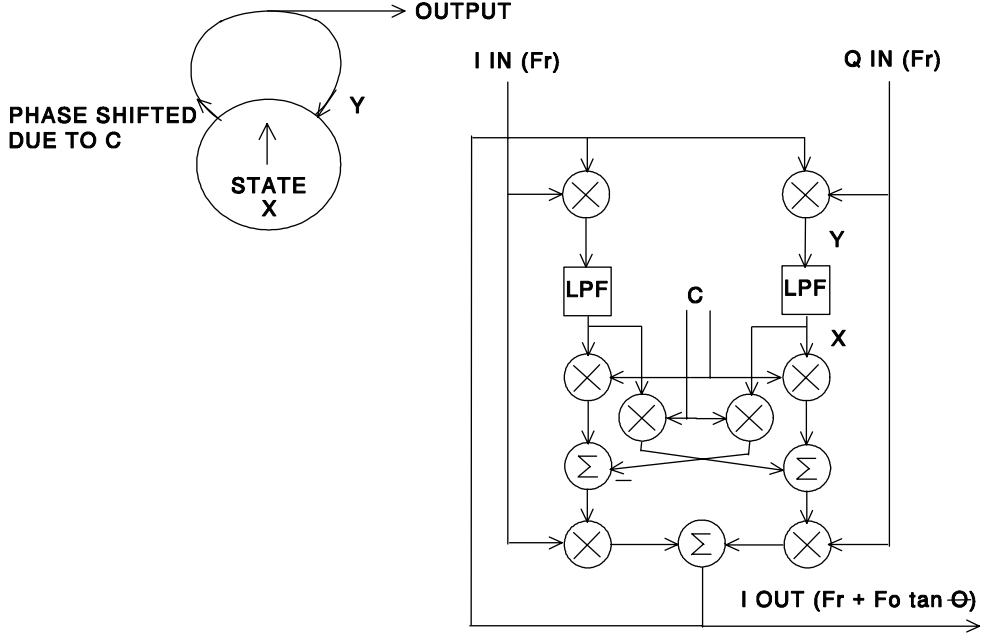
Figure 5.1: Circuit for single feedback oscillator convergence analysis.

The next step is to change to polar coordinates. Letting

$$x = ae^{j\alpha} \tag{54}$$

$$c = de^{j\theta}, \tag{55}$$

we can rewrite the dynamics as

$$\frac{1}{\omega_0}\dot{a} = -a + r_\beta(da)\cos\theta \tag{56}$$

$$\frac{1}{\omega_0}\dot{\alpha} = \frac{1}{a}r_\beta(da)\sin\theta. \tag{57}$$

Now, we need to make some assumptions on the sigmoidal function $r_\beta(\cdot)$. First, assume that the parameter β simply multiplies the argument of $r_\beta(\cdot)$, i.e.,

$$r_\beta(a) = r(\beta a) \quad \forall a, \beta \in \Re, \quad a, \beta \geq 0. \tag{58}$$

Second, $r(\cdot)$ must be strictly monotone increasing with $r(0) = 0$. Third, we will assume for convenience that $r(\cdot) \in C^\infty$. Finally, we require, as in section 2.4, that a function $h(\cdot)$ exist

satisfying

$$\begin{aligned}
\lim_{a \to \infty} \frac{h(a)}{r^2(a)} &= \infty, \\
\frac{\partial h}{\partial a} &= ar'(a), \text{ and} \\
h(0) &= \text{constant.}
\end{aligned} \tag{59}$$

These assumptions on $r_\beta(\cdot)$, which are not overly restrictive, are required for the following convergence analysis, which is used to conclude that the magnitude a of x converges to an equilibrium value regardless of initial conditions.

To prove convergence of the oscillator output amplitude, define the Lyapunov function

$$V(a) = -\frac{1}{2} r(\beta da)^2 \cos \theta + h(\beta da). \tag{60}$$

We first observe that our assumptions on $r(\cdot)$ imply that V is radially unbounded in its argument a (recall that $V(a)$ is radially unbounded in its argument a if $V(a) \to \infty$ as $a \to \infty$). Next, calculating $\dot{V}(a) = \frac{\partial V}{\partial a} \dot{a}$, we obtain

$$\begin{aligned}
\frac{\partial V}{\partial a} &= -\beta d r'(\beta da) r(\beta da) \cos \theta + \beta \frac{\partial h}{\partial a} \\
&= -\beta d r'(\beta da)[-a + r(\beta da) \cos \theta] \tag{61} \\
\dot{V}(a) &= \frac{\partial V}{\partial a} \dot{a} \\
&= -\beta d r'(\beta da)[-a + r(\beta da) \cos \theta]^2. \tag{62}
\end{aligned}$$

The assumptions on $r(\cdot)$ are sufficient to conclude that $\dot{V}(a) \leq 0 \;\; \forall a$, and $\dot{V}(a) = 0$ if and only if

$$-a + r(\beta da) \cos \theta = 0, \tag{63}$$

which holds at a point $x = ae^{j\alpha}$ if and only if it is an equilibrium point of the dynamics. (The singularity in the polar change of coordinates poses no problem because it is easy to see that the origin is an equilibrium point. For the circuit to work as an oscillator, we will want the equilibrium point at the origin to be unstable.) Combining the radial unboundedness of $V(a)$, the fact that $\dot{V}(a) \leq 0$ and $\dot{V}(a) = 0$ only at equilibrium points, and the observation that in fact

28

the dynamics for a actually follow the negative gradient of $V(a)$, we can conclude by the same arguments as in the previous convergence analyses that a converges to an equilibrium value.

5.2 Example: Continuous Wavelet Transform Circuit

5.2.1 Overview of the Continuous Wavelet Transform Application

The continuous wavelet transform (CWT) is currently seen as a potential alternative to digital signal wavelet processing in certain application areas in which the digital approach is too slow for real-time processing. Passive monitoring of the electromagnetic environment, radar systems, communications, and data compression are examples of potential application areas for the continuous wavelet transform.

An analog (e.g. microelectronic) CWT approach is based on the idea that the CWT can be realized using a bank of bandpass filters. Furthermore, because resolution in the time domain as well as in the frequency domain is intrinsically important for the CWT, the bandpass filters can be second-order, the lowest order possible for a bandpass filter.

Within a CWT system, there are two uses envisioned for microelectronic oscillator circuits. First, bandpass detectors implemented in the form of synchronous receivers require reference frequencies to be available to mix with the receiver input signal. As a reference frequency generator, the feedback oscillator circuit would be operating in its steady-state mode of operation.

The second CWT use for the microelectronic oscillator circuit would be to generate an approximation to the wavelet corresponding to the bandpass filter impulse response functions. The impulse response of a second-order bandpass filter is a burst at the center frequency of the filter with an exponentially decaying envelope whose time constant is related to the bandpass filter bandwidth. The transient response of the single feedback oscillator circuit is a burst at a frequency determined by design and with an exponentially growing envelope. Therefore, the bandpass filter with the same center frequency and bandwidth corresponding to the exponential time constant of the envelope serves as a matched filter for the signal generated by the oscillator

circuit.

5.2.2 Design Equations for Steady-State Operation

Figure 5.2 shows the single feedback oscillator circuit acting as a quadrature reference frequency generator for a CWT system. The sigmoidal transfer characteristic is simply the input saturating characteristic of the multiplier which multiplies the feedback signal by the high-frequency reference input, and hence is not a distinct component. Furthermore, the low-pass filter is just a capacitor placed across the differential multiplier outputs, and the summers are simply nodes where currents combine. Therefore, the oscillator circuit really only consists of 10 multipliers, and it provides both I and Q output signals (90° out of phase).
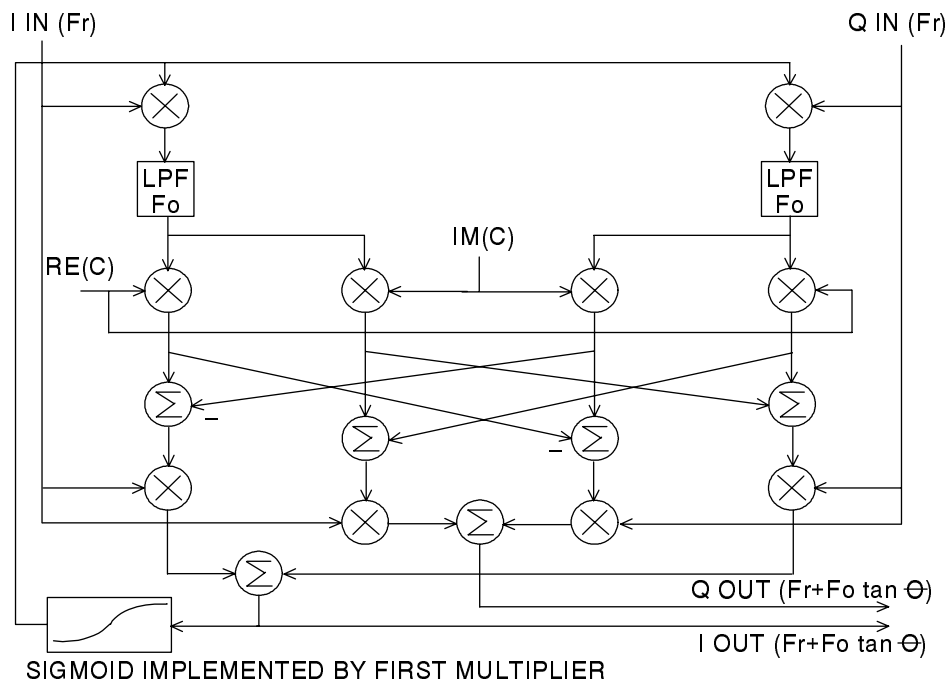

Figure 5.2: Single feedback oscillator frequency translator.

From the convergence analysis, we have the following dynamical equations for the oscillator

output:

$$\frac{1}{\omega_0}\dot{a} = -a + r_\beta(da)\cos\theta \tag{64}$$

$$\frac{1}{\omega_0}\dot{\alpha} = \frac{1}{a}r_\beta(da)\sin\theta. \tag{65}$$

The convergence analysis showed that the output amplitude a converged to a constant value, so that in steady state,

$$-a + r_\beta(da)\cos\theta = 0. \tag{66}$$

The steady-state equation for α, which represents the output signal phase with respect to the oscillator input frequency, then becomes

$$\frac{1}{\omega_0}\dot{\alpha} = \tan\theta, \tag{67}$$

where θ is assumed to be constant. Hence, the phase of the output signal, in steady state, advances at a constant rate given by $\omega_0\tan\theta$, which means that the output is frequency-shifted with repect to the input by $\omega_0\tan\theta$.

Thus, the output frequency of the oscillator circuit is given by the input frequency plus a term which depends on RC values (ω_0) times a term which is given by dc electrical inputs ($\tan\theta$). Therefore, if a number of oscillators which are identical except for geometrically scaled ω_0 values are driven with the same input frequency, the electrical input $c = de^{j\theta}$ can be used to correct for processing uncertanties in the ω_0 values. This is an important feature for a microelectronic circuit, because while ratios of time constants can be made relatively accurately on an IC, the absolute values have a very large uncertainty (as high as 50%). Furthermore, using feedback control, θ could be controlled to maintain the correct frequency ratios despite temperature changes.

Examination of the dynamics for a, equation (64), reveals that in order to destabilize the origin as an equilibrium point, $|\theta|$ must be sufficiently close to zero and βda must be large enough to overcome the decay term $-a$. The larger βd is, the larger $|\theta|$ can be, up to $\pi/2$, where the feedback is guaranteed to become negative. If $\theta = 0$, then the small signal gain through

31

the feedback loop must be greater than unity to prevent the oscillator output from decaying. In practice, there is a tradeoff between having a low feedback loop gain (to minimize power dissipation) and control authority through θ.

Even though the steady state output amplitude depends on both d and θ, the magnitude and polar angle of the complex input c, the output frequency only depends on θ and is independent of d. Therefore, the output frequency and amplitude can be tuned sequentially, another nice feature of this oscillator circuit.

5.2.3 Design Equations for transient operation

For the transient analysis of the circuit starting from an initial condition near the origin so that the output appears as a sine-wave burst with exponentially growing envelope, we need to reexamine the dynamical equations for a and α. If we assume that the slope of $r(\cdot)$ is unity at the origin, then the dynamics become, approximately,

$$\frac{1}{\omega_0}\dot{a} \;=\; (\beta d \cos\theta - 1)a \tag{68}$$

$$\frac{1}{\omega_0}\dot{\alpha} \;=\; \beta d \sin\theta. \tag{69}$$

Both the output frequency shift $\omega_0 \beta d \sin\theta$ and the time constant associated with the exponential growth, $1/[\omega_0(\beta d \cos\theta - 1)]$, depend on d and θ. The design equations for this case are thus two equations in two unknowns. In fact, since ω_0 is also a design parameter, many combinations of output frequency and envelope time constant can be obtained.

6. Implementation of Coupled Oscillator Circuits in Analog CMOS

To illustrate one approach for implementing the oscillator dynamics described in this work in analog CMOS hardware, consider the single feedback oscillator circuit of figure 5.2. The transistor-level circuit design basically comes down to deciding what type of four-quadrant multipliers to use for the ten multipliers appearing in the circuit, and then ensuring that the small-signal gain, sigmoidal nonlinearity, and lowpass filter time constant are correctly accounted for. The two multipliers whose outputs go to the low-pass filters are identical, the four multipliers

which perform the complex multiplication between the lowpass filter outputs and C are identical, and the four multipliers which produce the I and Q output signals are identical, so the design problem reduces to the design of only three distinct multiplier circuits.

Based on the success of the wide-range Gilbert multiplier circuits used in [19], the wide-range Gilbert multiplier circuit, shown in figure 6.1, would be a good choice for all three distinct multiplier circuits. However, different choices of transistor sizes are needed to provide the appropriate small-signal gain and saturating characteristic. Figure 6.2 shows multiplier star curves (from a PSPICE simulation) appropriate for the input-saturating multiplier. A fundamentally different approach for implementing the oscillator dynamics directly in the form of complex signals instead of as high-frequency real signals with different phases is described in [9].
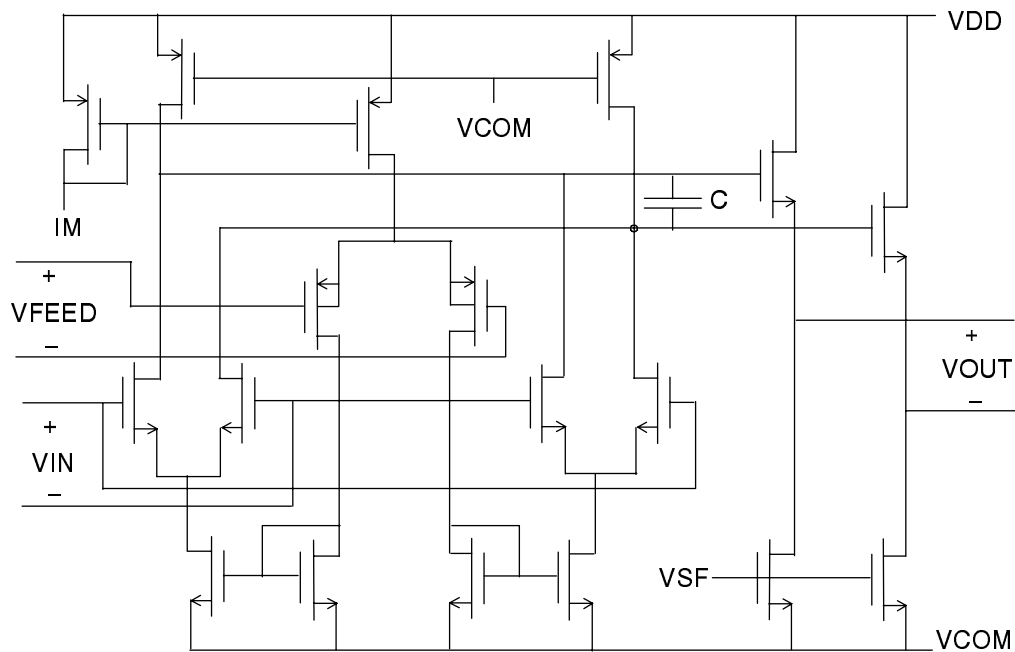

Figure 6.1: Wide-range Gilbert multiplier circuit.

Figure 6.2: Simulated star curves for multiplier with saturating input characteristic.

7. Conclusion

To summarize, convergence results for a class of networks of nonlinear coupled oscillators (or directional units, depending on the point of view taken) have been presented. Physical motivation has been given for the simplest network considered, but the convergence results for the rest of the networks are based solely on the adaptability of the original Lyapunov function arguments to the various networks.

The first modification to the fixed-weight network was the adaptively controlled network, which might be of interest for hierarchical control in systems with both local and global feedback. The second modification was the incorporation of external control inputs to the coupled oscillator network, and the example discussed was a pair of coupled oscillators for correcting for the feedback path phase shift of a complex LMS loop for adaptive filter applications. The third modification yielded a single oscillator with feedback through a complex weight, producing a circuit of potential interest for continuous wavelet transform applications. Analog CMOS implementation of the coupled oscillator dynamics was also briefly discussed.

This work represents a first attempt at applying a particularly basic form of coupled oscillator network to actual engineering problems. What the most useful oscillator network paradigms are, to what extent oscillator networks can be used in hierarchical control systems, and what the best implementation techniques are for high-speed analog circuit implementation all remain open questions.

References

[1] P.S. Krishnaprasad. "Motion Control and Coupled Oscillators," in press, *Motion, Control and Geometry: A Science and Technology Symposium*, National Academy of Sciences Press, Washington D.C., 1996.

[2] P. Baldi and R. Meir. Computing with Arrays of Coupled Oscillators: An Application to Preattentive Texture Discrimination. *Neural Computation*, 2:458-471, 1990.

[3] E. Lumer and B. Huberman. Binding Hierarchies: A Basis for Dynamic Perceptual Grouping. *Neural Computation*, 4:341-355, 1992.

[4] M. Mozer, R. Zemel, M. Behrmann, and C. Williams. Learning to Segment Images Using Dynamic Feature Binding. *Neural Computation*, 4:650-665, 1992.

[5] L. Shastri and V. Ajjanagadde. From simple associations to systematic reasoning: A Connectionist Representation of Rules, Variables, and Dynamic Bindings using Temporal Synchrony. *Behavioral and Brain Sciences*, Vol. 16, No. 3, pp. 417-494, 1993.

[6] A.H. Cohen. "Evolution of the Vertebrate Central Pattern Generator for Locomotion", in A.H. Cohen, S. Rossignol, and S. Grillner eds. *Neural Control of Rythmic Movements in Vertebrates*, John Wiley and Sons, Inc., New York, pp. 129-166, 1988.

[7] C.M. Gray. "Synchronous Oscillations in Neuronal Systems: Mechanisms and Functions", *Journal of Computational Neuroscience*, vol. 1, nos. 1/2, pp. 11-38, 1994.

[8] R. Zemel, C. Williams, and M. Mozer. Lending direction to neural networks. *Neural Networks*, 8:503-512, 1995.

[9] E. Justh. Convergence Analysis of a Class of Networks of Nonlinear Coupled Oscillators. Institute for Systems Research M.S. Thesis report, MS 94-11, 1994.

[10] E.W. Justh and P.S. Krishnaprasad, "Convergence Analysis of a Class of Networks of Nonlinear Coupled Oscillators." *Proceedings of the 34th IEEE Conference on Decision and Control*, pp. 1284-1289, 1995.

[11] P. Liao and R.A. York, "A New Phase-Shifterless Beam-Scanning Technique Using Arrays of Coupled Oscillators." *IEEE Transactions on Microwave Theory and Techniques,* Vol. 41, No. 10, Oct. 1993.

[12] T. Endo and K. Takeyama, "A Neural Network Using Oscillators." *Electronics and Communications in Japan, Part 3*, Vol. 75, Iss. 5, pp. 51-59, 1992.

[13] K.V. Mardia. *Statistics of Directional Data.* New York: Academic Press, 1972.

[14] H. Khalil. *Nonlinear Systems.* New York: Macmillan Publishing Co., 1992.

[15] E. Fischer. *Intermediate Real Analysis.* New York: Springer-Verlag, 1983.

[16] S. Lefschetz. *Differential Equations: Geometric Theory 2nd Ed.* New York: Wiley Interscience, 1963.

[17] E.D. Sontag, "Feedback stabilization of nonlinear systems." *Robust Control of Linear Systems and Nonlinear Control. Proceedings of the International Symposium MTNS-89 Vol. II*, pp. 61-81, 1990.

[18] B. Widrow and S.D. Stearns, *Adaptive Signal Processing.* Englewood Cliffs, NJ: Prentice-Hall, 1985.

[19] F.J. Kub and E.W. Justh, "Analog CMOS Implementation of High Frequency Least Mean Square Error Learning Circuits," *IEEE Journal of Solid State Circuits,* Vol. 30, No. 12, pp. 1391-1398, 1995.